

Simultaneous Border-Collision and Period-Doubling Bifurcations

D.J.W. Simpson and J.D. Meiss*
 Department of Applied Mathematics
 University of Colorado
 Boulder, CO 80309-0526

November 20, 2018

Abstract

We unfold the codimension-two simultaneous occurrence of a border-collision bifurcation and a period-doubling bifurcation for a general piecewise-smooth, continuous map. We find that, with sufficient non-degeneracy conditions, a locus of period-doubling bifurcations emanates non-tangentially from a locus of border-collision bifurcations. The corresponding period-doubled solution undergoes a border-collision bifurcation along a curve emanating from the codimension-two point and tangent to the period-doubling locus here. In the case that the map is one-dimensional local dynamics are completely classified; in particular, we give conditions that ensure chaos.

Piecewise-smooth, continuous maps are used to model nonsmooth physical situations with discrete-time inputs, and also arise as Poincaré maps in a variety of piecewise-smooth, systems of ordinary differential equations. Frequently a period-doubling bifurcation is the cause for a critical change in dynamics of a map producing a physically important period-doubled solution. A special situation arises in a piecewise-smooth, continuous map if this bifurcation occurs at a non-differentiable point in phase space. We show that soon after its creation, the period-doubled solution undergoes a border-collision bifurcation. Beyond this bifurcation the period-doubled solution may persist but the solution may also immediately become chaotic.

1 Introduction

Piecewise-smooth systems are currently being utilized in a wide variety of fields to model physical systems involving a discontinuity or sudden change. Examples include electrical circuits with a switching component such as a diode or a transistor [1, 2, 3], vibro-impacting

*D. J. W. Simpson and J. D. Meiss gratefully acknowledge support from NSF grant DMS-0707659.

systems and systems with friction [4, 5, 6, 7, 8], and optimization in economics [9, 10, 11]. In this paper we study discrete-time, piecewise-smooth systems that are everywhere continuous.

A map

$$x_{n+1} = F(x_n) , \tag{1}$$

is *piecewise-smooth continuous* if $F : \mathbb{R}^N \rightarrow \mathbb{R}^N$ is everywhere continuous but non-differentiable on codimension-one boundaries called *switching manifolds*. The collision of an invariant set with a switching manifold under parameter variation of (1) may produce a bifurcation that cannot occur in smooth systems. When the invariant set is a fixed point and a bifurcation occurs, the bifurcation is called a *border-collision bifurcation*.

Border-collision bifurcations may be analogous to familiar smooth bifurcations, such as saddle-node and period-doubling bifurcations. Alternatively they may be very complex. For instance a chaotic attractor may be generated at a border-collision bifurcation, even if the map is only one-dimensional [12]. In two or more dimensions, a complete classification of all possible dynamical behavior local to a border-collision bifurcation is yet to be determined, see for instance [13, 14, 15, 16, 17].

At a border-collision bifurcation a fixed point, x^* , lies on a switching manifold. Due to the lack of differentiability the stability multipliers associated with x^* are not well-defined. However, the switching manifold locally divides phase space into regions where the map has different smooth components; by continuity x^* is a fixed point of each component and, restricted to each component, associated multipliers of x^* are well-defined. Typically x^* will be a hyperbolic fixed point of each component. A special situation arises when x^* is non-hyperbolic in at least one component.

Under the assumption that the border-collision bifurcation occurs at a smooth point on a single switching manifold, there are exactly two smooth map components (half-maps), in some neighborhood. Consider the situation that x^* is hyperbolic in one half-map but non-hyperbolic in the other half-map. Then there are three codimension-two cases to consider; namely that on the non-hyperbolic side, x^* has an associated multiplier 1, a multiplier -1 or a complex conjugate pair of multipliers, $e^{\pm 2\pi i\omega}$. These correspond to the simultaneous occurrence of a border-collision bifurcation with a saddle-node bifurcation, a period-doubling bifurcation and a Neimark-Sacker bifurcation, respectively. Unlike a generic border-collision bifurcation, in each codimension-two case linear terms of the half-maps are insufficient to describe all local dynamical behavior.

For the first case, generically a locus of saddle-node bifurcations emanates from the codimension-two, border-collision bifurcation which in a two-parameter bifurcation diagram is a curve tangent to a locus of border-collision bifurcations [18] (see [19] for the continuous-time analogue). The third case may be very complicated and is left for future work. The precise nature of local bifurcations may depend on the rationality of ω . A recent analysis of these situations in a general piecewise-smooth map is given in [20]. The purpose of the present paper is to determine generic dynamical behavior of (1) local to the codimension-two border-collision bifurcation of the second case.

The coincidence of border-collision and period-doubling has been observed in real-world systems. Recall that a corner collision in a Filippov system provides an example of a border-collision bifurcation in a map [21]. In [22, 23] the authors describe the coincidence of a corner collision with period-doubling in a Filippov model of a DC/DC power converter.

Grazing-sliding (which also corresponds to a piecewise-smooth, continuous Poincaré map, see [24]) and period-doubling have been seen to occur simultaneously in a model of a forced, dry-friction oscillator [25].

In the next section we introduce a piecewise form for (1) suitable for the ensuing analysis and compute its fixed points. In §3 we unfold the codimension-two situation for the case that the map is one-dimensional. Here all local dynamical behavior is determined. We find there are essentially six distinct, generic, unfolding scenarios though each exhibit the same basic bifurcation curves. When the map is of a dimension greater than one we prove that the same basic bifurcation curves exist but do not classify all possible local dynamics, §4. Finally §5 gives conclusions.

2 Formulization of the codimension-two point and setup

We wish to explore local dynamical behavior near an arbitrary border-collision bifurcation of (1). We restrict ourselves to a neighborhood in both phase space and parameter space of the border-collision bifurcation within which we assume the border-collision bifurcation occurs on an isolated C^l switching manifold and that away from the switching manifold, F is C^k . Then, via coordinate transformations similar to those given in [26], we may assume the border-collision bifurcation occurs at the origin, $x = 0$, when a parameter, μ , is zero, and that to order l the switching manifold is simply the plane $e_1^\top x = 0$. In this paper we are not concerned with effects due to a nonsmooth switching manifold (for studies of various piecewise-smooth systems involving a non-differentiable switching manifold, see, for instance, [21, 27, 28, 29]). For this reason we assume l is sufficiently large to not affect local dynamics and for simplicity assume the switching manifold is exactly the plane $e_1^\top x = 0$.

For convenience we denote the first component of the N -dimensional vector, x , by s , i.e.

$$s = e_1^\top x .$$

Let η be a second map parameter, independent of μ . Then we are interested in local dynamics of

$$x_{n+1} = f(x_n; \mu, \eta) = \begin{cases} f^{(L)}(x_n; \mu, \eta), & s_n \leq 0 \\ f^{(R)}(x_n; \mu, \eta), & s_n \geq 0 \end{cases} , \quad (2)$$

where

$$f^{(i)}(x; \mu, \eta) = \mu b(\mu, \eta) + A_i(\mu, \eta)x + O(|x|^2) + o(k) , \quad (3)$$

is C^k for $i = L, R$. Here $b \in \mathbb{R}^N$ and A_L and A_R are $N \times N$ matrices which, by the assumption of continuity of (2), are identical in their last $N - 1$ columns. Throughout this paper we use the notation $O(k)$ [$o(k)$] to denote terms that are order k or larger [larger than order k] in all variables and parameters of a given expression. We refer to $f^{(L)}$ as the left half-map and $f^{(R)}$ as the right half-map.

Let us first determine fixed points of (2). Assume for the moment that for some η , 1 is not an eigenvalue of each $A_i(0, \eta)$. Then near $(x; \mu) = (0; 0)$, each half-map, $f^{(i)}$, has a unique fixed point

$$x^{*(i)}(\mu, \eta) = (I - A_i(0, \eta))^{-1}b(0, \eta)\mu + O(\mu^2) . \quad (4)$$

Recall that the adjugate of any matrix X , $\text{adj}(X)$, obeys $\text{adj}(X)X = \det(X)I$ [30, 31]. Since A_L and A_R can differ in only the first column, it follows that the first row of $\text{adj}(I - A_L)$ and of $\text{adj}(I - A_R)$ are identical. We denote this row by ϱ^\top :

$$\varrho^\top \equiv e_1^\top \text{adj}(I - A_L) = e_1^\top \text{adj}(I - A_R). \quad (5)$$

Multiplication of (4) by e_1^\top on the left yields

$$s^{*(i)}(\mu, \eta) = \frac{\varrho^\top b}{\det(I - A_i)} \Big|_{\mu=0} \mu + O(\mu^2), \quad (6)$$

where $s^{*(i)}$ denotes the first component of $x^{*(i)}$.

The point $x^{*(L)}$ is a fixed point of the piecewise-smooth map (2) and said to be *admissible* (that is, a fixed point of (2)) whenever $s^{*(L)} \leq 0$, otherwise it is said to be *virtual*. Similarly $x^{*(R)}$ is admissible exactly when $s^{*(R)} \geq 0$. The condition

$$\varrho^\top b|_{\mu=0} \neq 0, \quad (7)$$

ensures that the parameter μ “unfolds” the border-collision; we will assume this nondegeneracy condition holds.

Let us briefly review Feigin’s classification of border-collision bifurcations by the relative admissibility of fixed points and two-cycles (refer to [32] for further details). If $I - A_L(0, \eta)$ and $I - A_R(0, \eta)$ are both nonsingular and (7) is satisfied, for small μ each $x^{*(i)}$ is admissible when $\mu = 0$ and for one sign of μ . Let σ_i^+ [σ_i^-] denote the number of real eigenvalues of $A_i(0, \eta)$ that are greater than 1 [less than -1]. By (6), if $\sigma_L^+ + \sigma_R^+$ is even, $x^{*(L)}$ and $x^{*(R)}$ are admissible for different signs of μ . In this case as μ is varied through zero a single fixed point effectively *persists*. If instead $\sigma_L^+ + \sigma_R^+$ is odd, $x^{*(L)}$ and $x^{*(R)}$ are admissible for the same sign of μ ; at $\mu = 0$ the two fixed points collide and annihilate in a *nonsmooth fold bifurcation*. Furthermore if $I - A_L(0, \eta)A_R(0, \eta)$ is nonsingular, -1 is not an eigenvalue of $A_L(0, \eta)$ and $A_R(0, \eta)$, and $\sigma_L^- + \sigma_R^-$ is odd, then a two-cycle of (2) (that collapses to the origin as $\mu \rightarrow 0$) is admissible for one sign of μ , whereas if $\sigma_L^- + \sigma_R^-$ is even, no such two-cycle exists.

When $\mu = 0$, the origin is a fixed point of (2) that lies on the switching manifold, $s = 0$. For small $\mu \neq 0$, stability of, and dynamics local to, the fixed point, $x^{*(i)}$, are determined by the eigenvalues of $A_i(0, \eta)$. In nondegenerate situations the eigenvalues of the matrices $A_i(0, \eta)$ completely determine dynamics local to the border-collision bifurcation at $\mu = 0$. A special situation arises whenever either $A_L(0, \eta)$ or $A_R(0, \eta)$, has an eigenvalue that lies on the unit circle. Without loss of generality we may assume the former matrix has an eigenvalue on the unit circle when $\eta = 0$. In this situation a local smooth bifurcation may occur for the left half-map, $f^{*(L)}$, at $\mu = \eta = 0$. The nature of the smooth bifurcation is determined by nonlinear terms, consequently such terms are important to the border-collision bifurcation.

The remainder of this paper is an analysis of the case that -1 is an eigenvalue of $A_L(0, 0)$.

3 Unfolding in one dimension

We begin by treating the one-dimensional case, that is, $x = s \in \mathbb{R}$. Then the map (2) may be written as

$$x_{n+1} = \begin{cases} f^{(L)}(x_n; \mu, \eta), & x_n \leq 0 \\ f^{(R)}(x_n; \mu, \eta), & x_n \geq 0 \end{cases}. \quad (8)$$

We assume that the two smooth components of the map are at least C^3 (i.e. $k \geq 3$) and write them as

$$\begin{aligned} f^{(L)}(x; \mu, \eta) &= \mu b(\mu, \eta) + a_L(\mu, \eta)x + p(\mu, \eta)x^2 + q(\mu, \eta)x^3 + o(x^3), \\ f^{(R)}(x; \mu, \eta) &= \mu b(\mu, \eta) + a_R(\mu, \eta)x + O(x^2). \end{aligned} \quad (9)$$

The map (8) has a border-collision bifurcation at $\mu = 0$. We assume that the codimension-two situation of interest occurs at $\mu = \eta = 0$, that is $a_L(0, 0) = -1$. In order for parameters μ and η to unfold the bifurcation therefore we require $b(0, 0) \neq 0$ (by (7)) and $\frac{\partial a_L}{\partial \eta}(0, 0) \neq 0$. For simplicity we assume appropriate scalings upon μ and η have been performed such that these values are both 1 as stated in the following theorem.

Theorem 1.

Consider (8) with (9) and suppose

- i) $a_L(0, 0) = -1$ (singularity condition),
- ii) $b(0, 0) = 1$ (border-collision non-degeneracy condition),
- iii) $\frac{\partial a_L}{\partial \eta}(0, 0) = 1$ (transversality condition).

Let

$$a_0^{(R)} = a_R(0, 0), \quad (10)$$

$$c_0 = p^2(0, 0) + q(0, 0). \quad (11)$$

Then there exists $\delta > 0$ such that the left half-map restricted to the neighborhood

$$\mathcal{N} = \left\{ (x; \mu, \eta) \mid |x|, |\mu|, |\eta| < \delta \right\} \quad (12)$$

has a unique fixed point given by a C^k function, $x^{*(L)}(\mu, \eta) = \frac{1}{2}\mu + O(2)$, and there exist unique, C^{k-1} functions $h_1, h_2 : \mathbb{R} \rightarrow \mathbb{R}$ that satisfy

$$h_1(\mu) = - \left(\frac{\partial a_L}{\partial \mu} + p \right) \Big|_{\mu=\eta=0} \mu + O(\mu^2), \quad (13)$$

$$h_2(\mu) = h_1(\mu) - \frac{c_0}{4}\mu^2 + o(\mu^2), \quad (14)$$

such that

- 1) when $\mu < 0$, $x^{*(L)}(\mu, h_1(\mu))$ has an associated multiplier of -1 , and if $c_0 \neq 0$ the curve $\eta = h_1(\mu)$ corresponds to a locus of admissible, period-doubling bifurcations of $x^{*(L)}$,
- 2) the origin belongs to a period-two orbit of $f^{(L)}$ on $\eta = h_2(\mu)$ that is admissible when $\mu < 0$,
- 3) if $a_0^{(R)} \neq \pm 1$ and $c_0 \neq 0$, then fixed points and two-cycles of (8) exist in the sectors shown in Fig. 1,

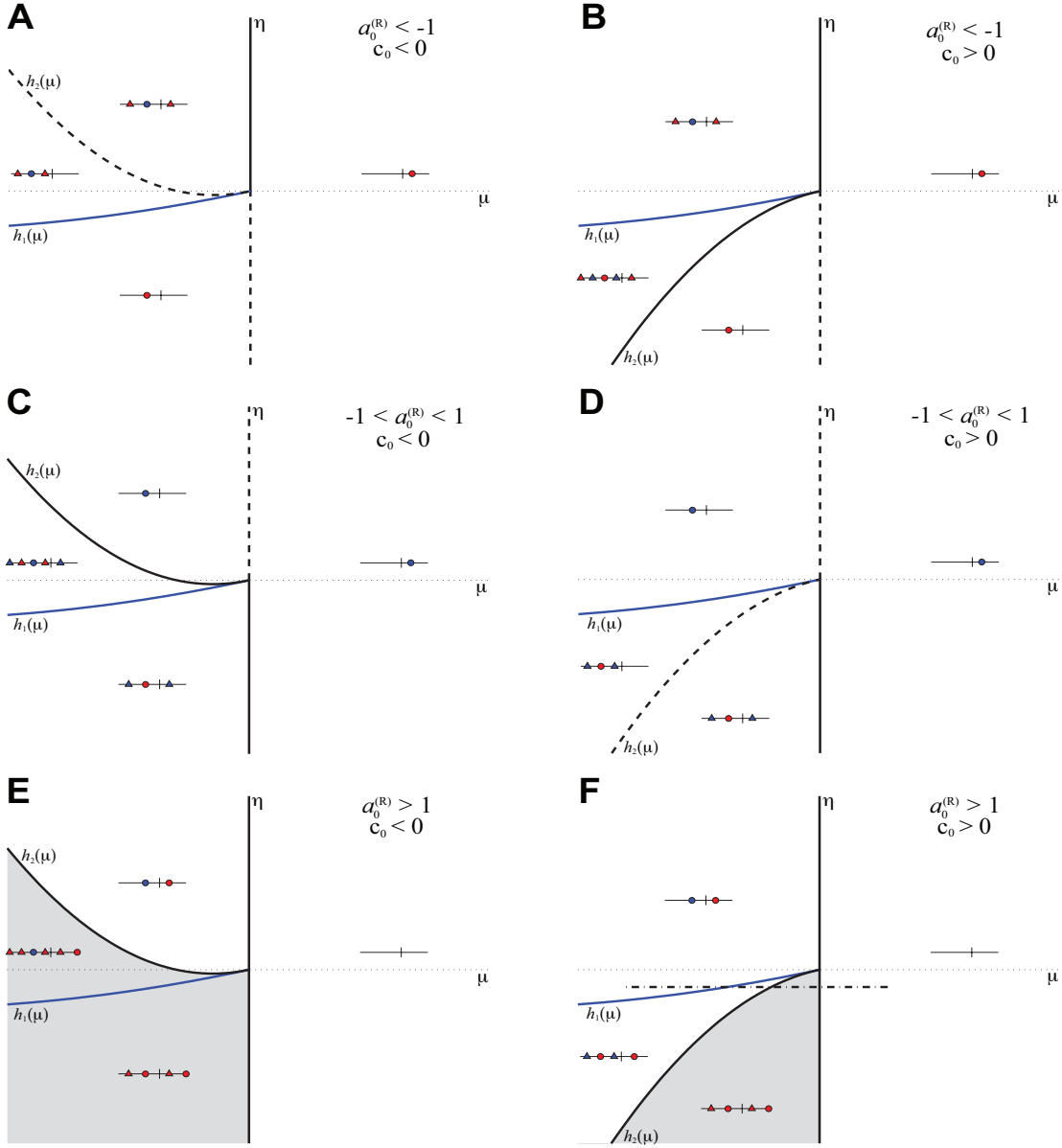


Figure 1: Sketches of bifurcation sets of (8) for different values of $a_0^{(R)}$ and c_0 , see Theorem 1. Blue curves correspond to loci of period-doubling bifurcations; black curves correspond to border-collisions and are shown dashed when no topological change occurs at the border-collision. Insets show phase portraits with circles used to denote fixed points and triangles used to denote points on two-cycles. These are blue when the solutions are stable and red otherwise. The small vertical lines denote the switching manifold. Chaotic dynamics occurs only for parameter values in the shaded regions; indeed, periodic solutions of a period higher than two only occur in these regions. The bifurcation diagram shown in Fig. 2 is taken along the dash-dot line segment of panel F.

- 4) if $a_0^{(R)} < 1$ or $\mu > 0$ or $\eta > h_2(\mu)$, (8) has no n -cycles for any $n \geq 3$ in \mathcal{N} ,
- 5) if $a_0^{(R)} > 1$ and $\mu < 0$ and $\eta < h_2(\mu)$, then (8) exhibits chaos in \mathcal{N} .

A proof of Theorem 1 is given in Appendix A. To facilitate the extension of Theorem 1 to higher dimensions in §4, the theorem is stated in a manner that yields a partial result when the non-degeneracy condition on the nonlinear terms, $c_0 \neq 0$, is not satisfied. The sign of c_0 determines the criticality of the period-doubling bifurcations.

Fig. 1 shows the six different bifurcation scenarios depending on the value of $a_0^{(R)}$ and the sign of c_0 that are predicted by the theorem. In each case the nature of the border-collision bifurcation at $\mu = 0$ for small $\eta \neq 0$ may be determined by referring to the well-understood, one-dimensional, piecewise-linear map

$$x_{n+1} = \begin{cases} \mu + a_L x_n, & x_n \leq 0 \\ \mu + a_R x_n, & x_n \geq 0 \end{cases}, \quad (15)$$

see for instance [12]. For example, along the positive η -axis in Fig. 1-A, we have $a_L \approx -1 + \eta > -1$ and $a_R < -1$, thus by Feigin's classification a single fixed point persists and a two-cycle is created that coexists with the left fixed point and is stable.

In panels E and F, along the negative η -axis we have $a_L \approx -1 + \eta < -1$ and $a_R > 1$. At points just to the left of the negative η -axis, both fixed points and a two-cycle are

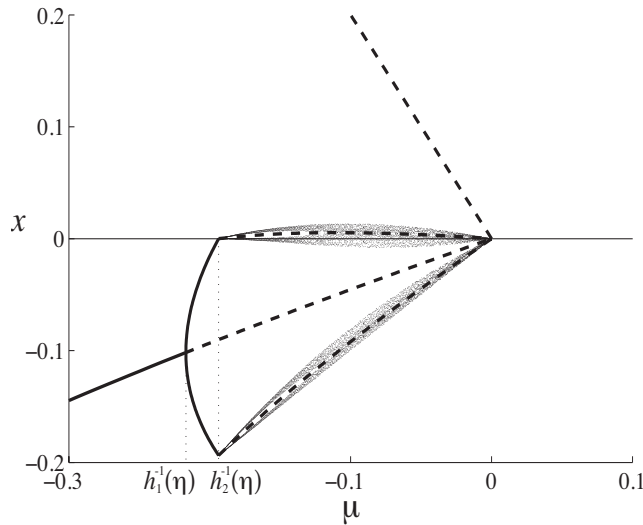


Figure 2: A bifurcation diagram for (8) when $b = 1$, $a_L = \eta - 1$, $a_R = \frac{3}{2}$, $p = -1$, $q = \frac{3}{2}$ and there are no additional higher order terms. The value of η is fixed at -0.25 . The parameters considered correspond to the dash-dot line segment shown in Fig. 1. Stable [unstable] fixed points and two-cycles are indicated by solid [dashed] curves. A supercritical period-doubling bifurcation occurs at $\mu = h_1^{-1}(\eta) \approx -0.2169$; a border-collision bifurcation of the period-doubled solution occurs at $\mu = h_2^{-1}(\eta) \approx -0.1937$. When $h_2^{-1}(\eta) < \mu < 0$ there exists a chaotic attracting set. When $\mu > 0$ there is no local attractor.

admissible and unstable. Forward orbits are attracted to a chaotic solution created at the border-collision bifurcation at $\mu = 0$. Unstable high period orbits are also generated at the border-collision bifurcation; these are of even period. To further illustrate the unfolding, Fig. 2 shows a bifurcation diagram corresponding to a one-parameter slice of Fig. 1-F. The chaotic attracting set collapses to the origin at $\mu = 0$ and to a two-cycle at $\mu = h_2^{-1}(\eta)$.

Two-cycles created in border-collision bifurcations at $\mu = 0$ consist of one point in each half-plane. In contrast, two-cycles created in period-doubling bifurcations along $\eta = h_1(\mu)$ lie entirely in the left half-plane. Along $\eta = h_2(\mu)$ these two orbits coincide and are given explicitly by $\{0, \mu b(\mu, h_2(\mu))\}$. The second iterate of (8) can be transformed into a map of the form (2) along $\eta = h_2(\mu)$, see (28). The resulting left and right period-two maps have multipliers $1 - c_0\mu^2 + o(\mu^2)$ and $-a_0^{(R)} + O(\mu)$ respectively. By Feigin's classification, four-cycles are born at $\eta = h_2(\mu)$ exactly when $a_0^{(R)} > 1$, i.e. in panels E and F of Fig. 1, though these are not shown.

4 Higher dimensions

We now analyze the codimension-two scenario in an arbitrary number of dimensions, i.e. $x \in \mathbb{R}^N$. Recall that for smooth systems the concept of dimension reduction by center manifold analysis allows bifurcations in systems of any number of dimensions to be transformed to their low dimensional normal forms. Unfortunately this technique cannot be applied here because (2) is not differentiable in a neighborhood of the bifurcation. However we can compute a center manifold of the C^k , left half-map. Assuming certain nondegeneracy conditions, we will show that the restriction of the left half-map to this center manifold yields a one-dimensional map that has the same form as the left half-map of (8) and satisfies the conditions (i)-(iii) of Theorem 1. Consequently the aspects of Theorem 1 that incorporate only the left half-map extend immediately to the same scenario in higher dimensions. That is, there exists a curve $\eta = h_1(\mu)$ along which period-doubling bifurcations occur and a curve $\eta = h_2(\mu)$ along which the two-cycle created at the period-doubling bifurcation collides with the switching manifold. The drawback of this approach is that we fail to describe dynamical behavior of (2) that occurs on both sides of the switching manifold.

Let us state our main result:

Theorem 2.

Consider the piecewise- C^k , continuous map (2) with (3) on \mathbb{R}^N and assume $N \geq 2$ and $k \geq 4$. Suppose that near $(\mu, \eta) = (0, 0)$, $A_L(\mu, \eta)$ has an eigenvalue $\lambda(\mu, \eta) \in \mathbb{R}$ with an associated eigenvector, $v(\mu, \eta)$. In addition, suppose

- i) $\lambda(0, 0) = -1$ is of algebraic multiplicity one and $A_L(0, 0)$ has no other eigenvalues on the unit circle,*
- ii) $\varrho^T(0, 0)b(0, 0) \neq 0$ (where ϱ^T is given by (5)),*
- iii) $\frac{\partial \lambda}{\partial \eta}(0, 0) = 1$,*
- iv) the first element of $v(0, 0)$ is nonzero, thus by scaling assume $e_1^T v(0, 0) = 1$,*

v) $\det(I - A_L(0, 0)A_R(0, 0)) \neq 0$.

Then, in the extended coordinate system $(x; \mu, \eta)$, there exists a C^{k-1} three-dimensional center manifold, W^c , for the left half-system that passes through the origin and is not tangent to the switching manifold at this point. Furthermore, $f^{(L)}|_{W^c}$, described in the coordinate system $(\hat{x}; \hat{\mu}, \hat{\eta}) = (s; \frac{2\sigma^T b}{\det(I-A_L)}|_{(0,0)}\mu, \eta)$, is given by the left half-map of (8) with “hatted variables” and the conditions (i)-(iii) of Theorem 1 will be satisfied.

If $c_0 \neq 0$ in Theorem 1 (where c_0 is computed for $f^{(L)}|_{W^c}$), then along a C^{k-2} curve, $\hat{\eta} = h_1(\hat{\mu})$, the unique fixed point of the left half-map near the origin undergoes a period-doubling bifurcation that is admissible when $\hat{\mu} < 0$, and along a C^{k-2} curve, $\hat{\eta} = h_2(\hat{\mu})$, the period-doubled solution collides with the switching manifold. These two curves intersect and are tangent at $\hat{\mu} = \hat{\eta} = 0$. Moreover, a unique two-cycle consisting of one point on each side of the switching manifold exists for small μ and η . This cycle is admissible exactly when $\hat{\mu} \leq 0$ and $\hat{\eta} \leq \text{sgn}\left(\frac{\det(I-A_L)\frac{\partial}{\partial \eta}\det(I+A_L)}{\det(I-A_L A_R)}\bigg|_{(0,0)}\right) h_2(\hat{\mu})$.

A proof is given in Appendix B. Conditions (i)-(iii) are analogous to the first three conditions of Theorem 1. Condition (iv) is a non-degeneracy condition that ensures the period-doubled cycles collide with the switching manifold in the generic manner. If this condition is not satisfied, a higher codimension situation that involves linear separation between $h_1(\mu)$ and $h_2(\mu)$ may arise. Finally condition (v) is necessary to ensure that non-degenerate, two-cycles are created at $\mu = 0$.

Theorem 2 essentially predicts the same basic bifurcation structure as Theorem 1. The relative position of h_1 and h_2 and the criticality of the period-doubling bifurcation are determined by the sign of c_0 . In one dimension, c_0 is a simple function of coefficients of nonlinear terms of the left half-map (11). To obtain the value of c_0 in higher dimensions, one may derive an expression for the restriction of the left half-map to the center manifold, then apply the one dimensional result. This is done for an example below. An explicit expression for c_0 in N dimensions is probably too complicated to be of practical use.

To illustrate Theorem 2 consider the following map on \mathbb{R}^2 using $x = (s, y)$:

$$\begin{aligned} s' &= -\frac{1}{2}\mu - \frac{1}{2}s + y, \\ y' &= \frac{1}{3}s - \frac{1}{6}|s| - \frac{3}{2}\eta s + \frac{1}{4}s^2. \end{aligned} \tag{16}$$

This map is easily rewritten in the piecewise form (2) with (3) and as we will show (16) satisfies the assumptions of Theorem 2. When $\mu = 0$ the origin is a fixed point of (16) which lies on the switching manifold, $s = 0$. Consequently the η -axis corresponds to a locus of border-collision bifurcations.

Fig. 3 shows a two-dimensional bifurcation diagram of (16) near $\mu = \eta = 0$. Period-doubling bifurcations occur along $\eta = h_1(\mu)$ and the period-doubled solutions undergo border-collision along $\eta = h_2(\mu)$; these curves are given explicitly by

$$\begin{aligned} h_1(\mu) &= -\frac{1}{6}\mu - \frac{1}{48}\mu^2 + O(\mu^3), \\ h_2(\mu) &= -\frac{1}{6}\mu, \end{aligned} \tag{17}$$

(actually $h_1^{-1}(\eta) \equiv -6\eta - \frac{9}{2}\eta^2$). The curves are tangent at $\mu = \eta = 0$ as predicted by Theorem 2. Near this point the dynamics resemble Fig. 1C although there is an additional unstable two-cycle present that does not undergo bifurcation at $\mu = \eta = 0$. This two-cycle collides with the stable two-cycle born at $\mu = 0$ for small $\eta < 0$ along a locus of saddle-node bifurcations (shown red in Fig. 3). The saddle-node locus emanates from the η -axis at $\eta = \frac{-4+\sqrt{10}}{9} \approx -0.093$ which is where the stable two-cycle loses stability. Also a cusp bifurcation of period-two orbits occurs at $(\mu, \eta) = (-\frac{1}{18}, -\frac{1}{9})$.

A second simultaneous border-collision and period-doubling bifurcation occurs on the η -axis at $\eta = -\frac{2}{9}$. As predicted by Theorem 2 a locus of period-doubling bifurcations and border-collision bifurcations of the period-doubled solution emanate from the codimension-two point and are tangent to one another here. Locally the bifurcation set resembles Fig. 1A.

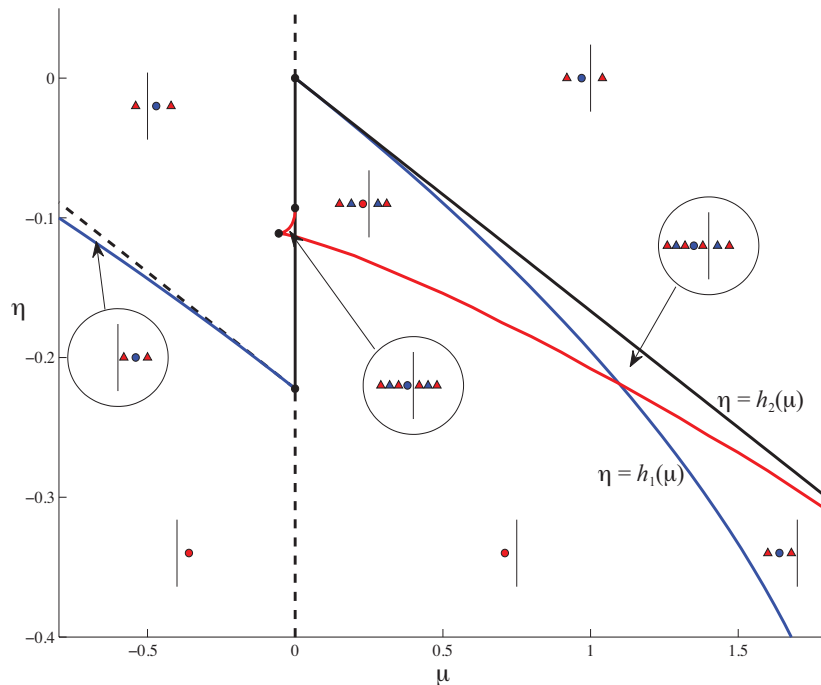


Figure 3: A bifurcation set of the two-dimensional, piecewise- C^∞ map (16). Border-collision bifurcations of fixed points and two-cycles are indicated by black curves which are dashed when no bifurcation occurs in a topological sense. Blue curves correspond to period-doubling bifurcations of a fixed point; red curves correspond to saddle-node bifurcations of a two-cycle. As in Fig. 1, schematics showing fixed points and two-cycles are included. Dynamics local to the codimension-two points $(\mu, \eta) = (0, 0)$ and $(0, -\frac{2}{9})$ are described by Theorem 2.

We now perform calculations to verify the details of Theorem 2 for the map (16) near $\mu = \eta = 0$. Here $\varrho^\top(0, 0) = [1, 1]$, $b(0, 0) = [-\frac{1}{2}, 0]^\top$ and $\det(I - A_L(0, 0)) = 1$, thus $\hat{\mu} = -\mu$ and therefore $h_1(\mu)$ corresponds to admissible solutions when $\mu > 0$, matching Fig. 3. Also, $\frac{\partial}{\partial \eta} \det(I + A_L) \Big|_{(0,0)} = \frac{3}{2}$ and $\det(I - A_L(0, 0)A_R(0, 0)) = \frac{1}{6}$, hence by the last statement of Theorem 2, two-cycles born on h_2 with points on each side of the switching manifold are admissible below h_2 , in agreement with Fig. 3.

Using a series expansion (see also the proof of Theorem 2), one finds that the left half-map of (16) restricted to the center manifold is given by

$$s' = \hat{\mu} - s + \frac{1}{2}s^2 - \frac{2}{3}\hat{\mu}s + \eta s + \frac{1}{3}\hat{\mu}^2 - 2\hat{\mu}\eta - \frac{1}{3}s^3 + \dots$$

Here the coefficient $-(\frac{\partial a_L}{\partial \hat{\mu}} + p)\Big|_{(0,0)}$, given in Theorem 1, is equal to $\frac{1}{6}$. Also $c_0 = -\frac{1}{12}$. Thus $h_1(\mu) = -\frac{1}{6}\mu + O(\mu^2)$ and $h_2(\mu) - h_1(\mu) = \frac{1}{48}\mu^2 + O(\mu^3)$ matching the explicit results given above.

5 Conclusions

A two-parameter bifurcation diagram provides a useful and concise picture of the behavior of a dynamical system near a codimension-two point. Loci or curves in such diagrams correspond to codimension-one phenomena. The intersection of two or more bifurcation curves at a codimension-two point occurs in a manner that is generally determined by the corresponding codimension-one bifurcations. We have shown that for a general piecewise-smooth, continuous map, loci of border-collision and period-doubling bifurcations of a single fixed point generically intersect non-tangentially (unlike the analogous intersection of a border-collision bifurcation and a saddle-node bifurcation [18]). Moreover the period-doubled solution undergoes border-collision along a locus that emanates from the codimension-two point and is tangent to the period-doubling curve here.

We have determined all local dynamical phenomena that occurs when this scenario arises generically in a one-dimensional system. In particular we have shown exactly when chaotic dynamics may be generated. In higher dimensions border-collision bifurcations near the codimension-two point may in addition generate quasiperiodic solutions such as invariant circles or other more complicated orbits.

A Proof of Theorem 1

The theorem is proved in five steps. First, the function h_1 is calculated by finding where $x^{*(L)}$ has an associated multiplier of -1 . Second, h_2 is calculated from an expression for $f^{(L)2}$. Third, an explicit computation of the piecewise-smooth, second iterate map allows the border-collision bifurcation of the two-cycle that occurs along $\eta = h_2(\mu)$ to be classified. Finally, in steps four and five we prove parts (4) and (5) respectively.

Since $f^{(L)}$ (9) is C^k and $k \geq 3$, we can write

$$\begin{aligned} a_L(\mu, \eta) &= -1 + \alpha_1\mu + \eta + \alpha_3\mu^2 + \alpha_4\mu\eta + \alpha_5\eta^2 + o(2) , \\ b(\mu, \eta) &= 1 + \beta_1\mu + \beta_2\eta + O(2) , \\ p(\mu, \eta) &= \gamma_0 + \gamma_1\mu + \gamma_2\eta + o(1) , \\ q(\mu, \eta) &= \delta_0 + o(0) , \end{aligned} \tag{18}$$

where we have used hypotheses of the theorem to simplify the coefficients.

Step 1: Compute the function h_1 which corresponds to the existence of a fixed point of the left half-map with multiplier -1 .

By the implicit function theorem the left half-map has the fixed point

$$x^{*(L)}(\mu, \eta) = \frac{1}{2}\mu + k_1\mu^2 + k_2\mu\eta + k_3\eta^2 + O(3), \quad (19)$$

which is a C^k function of μ and η and locally satisfies $f^{(L)}(x^{*(L)}(\mu, \eta); \mu, \eta) - x^{*(L)}(\mu, \eta) \equiv 0$. By a second order expansion, it is determined that the scalar coefficients, k_i , have the values

$$\begin{aligned} k_1 &= \frac{\beta_1}{2} + \frac{\alpha_1}{4} + \frac{\gamma_0}{8}, \\ k_2 &= \frac{\beta_2}{2} + \frac{1}{4}, \\ k_3 &= 0. \end{aligned} \quad (20)$$

The multiplier associated with $x^{*(L)}(\mu, \eta)$ is found by substituting (19) into $D_x f^{(L)}(x; \mu, \eta)$ (see (9)). We obtain

$$\begin{aligned} D_x f^{(L)}(x^{*(L)}(\mu, \eta); \mu, \eta) &= -1 + (\alpha_1 + \gamma_0)\mu + \eta + \left(\alpha_3 + 2k_1\gamma_0 + \gamma_1 + \frac{3\delta_0}{4} \right) \mu^2 \\ &\quad + (\alpha_4 + 2k_2\gamma_0 + \gamma_2)\mu\eta + \alpha_5\eta^2 + o(2). \end{aligned} \quad (21)$$

The implicit function theorem implies that

$$h_1(\mu) = -(\alpha_1 + \gamma_0)\mu + l_1\mu^2 + o(\mu^2), \quad (22)$$

is a C^{k-1} function that locally satisfies $D_x f^{(L)}(x^{*(L)}(\mu, h_1(\mu)); \mu, h_1(\mu)) + 1 \equiv 0$, where l_1 is found by substituting (22) into (21),

$$l_1 = - \left(\alpha_3 + 2k_1\gamma_0 + \gamma_1 + \frac{3\delta_0}{4} \right) + (\alpha_4 + 2k_2\gamma_0 + \gamma_2)(\alpha_1 + \gamma_0) - \alpha_5(\alpha_1 + \gamma_0)^2. \quad (23)$$

When $c_0 \neq 0$, the existence of period-doubling bifurcations along $\eta = h_1(\mu)$ for small μ is verified by checking the three conditions of the standard theorem, see for instance [33]:

- i) (singularity) by construction, $D_x f^{(L)}(x^{*(L)}(\mu, h_1(\mu)); \mu, h_1(\mu)) \equiv -1$,
- ii) (transversality) $\left(\frac{\partial f^{(L)}}{\partial \eta} \frac{\partial^2 f^{(L)}}{\partial x^2} + 2 \frac{\partial^2 f^{(L)}}{\partial x \partial \eta} \right) \Big|_{\eta=h_1(\mu)} = 2 + O(\mu) \neq 0$,
- iii) (non-degeneracy) $\left(\frac{1}{2} \left(\frac{\partial^2 f^{(L)}}{\partial x^2} \right)^2 + \frac{1}{3} \frac{\partial^3 f^{(L)}}{\partial x^3} \right) \Big|_{\eta=h_1(\mu)} = 2c_0 + O(\mu) \neq 0$.

Consequently we have proved (1) of the theorem.

Step 2: Compute the function h_2 which corresponds to the existence of a period-two orbit of the left half-map at $x = 0$.

To determine h_2 , we compute the C^k function $f^{(L)^2}(0; \mu, \eta) = f^{(L)}(\mu b(\mu, \eta); \mu, \eta)$ which may be written as $f^{(L)^2}(0; \mu, \eta) = \mu g(\mu, \eta)$ where

$$g(\mu, \eta) = b(\mu, \eta) \left(1 + a_L(\mu, \eta) + \mu b(\mu, \eta) p(\mu, \eta) + \mu^2 b^2(\mu, \eta) q(\mu, \eta) \right) + o(2), \quad (24)$$

is C^{k-1} . Substitution of (18) into (24) produces

$$\begin{aligned} g(\mu, \eta) &= (\alpha_1 + \gamma_0)\mu + \eta + (\alpha_1\beta_1 + \alpha_3 + 2\beta_1\gamma_0 + \gamma_1 + \delta_0)\mu^2 \\ &\quad + (\beta_1 + \alpha_1\beta_2 + \alpha_4 + 2\beta_2\gamma_0 + \gamma_2)\mu\eta + (\beta_2 + \alpha_5)\eta^2 + o(2). \end{aligned} \quad (25)$$

The implicit function theorem implies that

$$h_2(\mu) = -(\alpha_1 + \gamma_0)\mu + l_2\mu^2 + o(\mu^2), \quad (26)$$

is a C^{k-1} function that locally satisfies $g(\mu, h_2(\mu)) \equiv 0$. By substituting (26) into (25) we deduce

$$\begin{aligned} l_2 &= -(\alpha_1\beta_1 + \alpha_3 + 2\beta_1\gamma_0 + \gamma_1 + \delta_0) + (\beta_1 + \alpha_1\beta_2 + \alpha_4 + 2\beta_2\gamma_0 + \gamma_2)(\alpha_1 + \gamma_0) \\ &\quad - (\beta_2 + \alpha_5)(\alpha_1 + \gamma_0)^2. \end{aligned} \quad (27)$$

Subtracting (23) from (27) produces (after algebraic simplification)

$$l_2 - l_1 = -\frac{\gamma_0^2 + \delta_0}{4},$$

which proves (14) in the statement of the theorem.

Step 3: *Determine all two-cycles to verify the phase portraits in Fig. 1.*

For small, fixed $\mu < 0$, the two-cycle generated in a period-doubling bifurcation at $\eta = h_1(\mu)$ undergoes a border-collision bifurcation when it collides with the switching manifold at $\eta = h_2(\mu)$. The stability and relative admissibility of two-cycles emanating from this border-collision bifurcation is found by determining a map of the form (15) that describes the bifurcation. Such a map may be obtained by computing the second iterate of (8) and replacing η with the new parameter

$$\hat{\eta} = \eta - h_2(\mu),$$

which controls the border-collision. Near $\hat{\eta} = 0$, when $\mu < 0$ period-two orbits are guaranteed to have one negative point, so we compute $f^{(L)} \circ f^{(L)}$ and $f^{(L)} \circ f^{(R)}$ which leads to

$$f^2(x; \mu, \hat{\eta}) = \begin{cases} (\mu + O(\mu^2))\hat{\eta} + (1 - c_0\mu^2 + o(\mu^2))x + O(|x, \hat{\eta}|^2), & x \leq 0 \\ (\mu + O(\mu^2))\hat{\eta} + (-a_0^{(R)} + O(\mu))x + O(|x, \hat{\eta}|^2), & x \geq 0 \end{cases} \quad (28)$$

A fixed point, $x^{*(LL)}$, of the left half-map of (28) corresponds to a two-cycle of (8) with both points negative-valued, when admissible. By (28), if $c_0 < 0$ [$c_0 > 0$], then $x^{*(LL)}$ is unstable and admissible when $\hat{\eta} < 0$ [stable and admissible when $\hat{\eta} > 0$]. Similarly, a fixed point, $x^{*(RL)}$ of the right half-map of (28) corresponds to a two-cycle of (8) comprised of two points with different signs, when admissible. If $|a_0^{(R)}| < 1$, then $x^{*(RL)}$ is stable, otherwise

it is unstable. Furthermore if $a_0^{(R)} < -1$ [$a_0^{(R)} > -1$], then $x^{*(RL)}$ is admissible when $\hat{\eta} > 0$ [$\hat{\eta} < 0$]. Lastly, since $a_0^{(R)} \neq -1$, the fixed point, $x^{*(RL)}$, is unique for small μ and η . Therefore the two-cycle created at $\mu = 0$ collides with the switching manifold at $\eta = h_2(\mu)$. These statements verify all two-cycles shown in Fig. 1.

Step 4: Show that f , (8), has no n -cycles with $n \geq 3$, verifying part (4).

Except when $a_0^{(R)} = 0$ our proof is founded on the knowledge that a one-dimensional map cannot have an n -cycle with $n \geq 3$ contained in an interval on which the map is monotone. For the special case $a_0^{(R)} = 0$ we used several additional logical arguments including the contraction mapping theorem.

Case I: $a_0^{(R)} < 0$.

In this case there exists $\delta > 0$ such that $\forall \mu, \eta \in [-\delta, \delta]$, f is decreasing on $[-\delta, \delta]$. Consequently f has no n -cycles with $n \geq 3$ on $[-\delta, \delta]$.

Case II: $a_0^{(R)} = 0$.

First we construct an interval containing the origin on which f is forward invariant. Since the two components of f are differentiable, there exists $\hat{\delta} > 0$ such that $\forall \mu, \eta, x \in [-\hat{\delta}, \hat{\delta}]$,

$$\left| \frac{\partial f^{(R)}}{\partial x} \right|, \left| \frac{\partial f^{(L)}}{\partial x} + 1 \right|, |b(\mu, \eta) - 1| \leq \frac{1}{3}.$$

Let $\delta = \frac{1}{8}\hat{\delta}$, let $I = [-4\delta, 8\delta]$ and assume $\mu, \eta \in [-\delta, \delta]$. Then $f(I) \subset I$ because for any $x \in I$, we may assume $x > 0$ when calculating a lower bound for $f(x)$: $f(x) \geq \mu b - \frac{1}{3}x \geq -\frac{4}{3}\delta - \frac{8}{3}\delta = -4\delta$, and we may assume $x < 0$ when calculating an upper bound: $f(x) \leq \mu b - \frac{4}{3}x \leq \frac{4}{3}\delta + \frac{4}{3}4\delta < 8\delta$.

If $\mu \geq 0$ then the image of any $x < 0$ under f is positive and since the right half-map is contracting and the slope of the left half-map is near -1 , f^2 is a contraction on I , indeed $|D_x f^2(x)| \leq \frac{4}{3} < 1$. By the contraction mapping theorem, iterates of f^2 approach a unique fixed point, which must be $x^{*(R)}$, therefore f cannot have an n -cycle with $n \geq 3$ on \mathcal{N} (12).

So we now assume $\mu < 0$. Recall that when $\eta = h_2(\mu)$, $f^{(L)^2}(0) = 0$, i.e. $f(0) = f^{(L)^{-1}}(0)$, and when $\eta > h_2(\mu)$, $f(0) > f^{(L)^{-1}}(0)$. Therefore if $\eta \geq h_2(\mu)$, see Fig. 4-A, the interval $[f^{(L)^{-1}}(0), 0]$ is forward invariant. Since f is monotone on the interval

$$J = [f(0), 0], \tag{29}$$

it contains no n -cycles with $n \geq 3$ here. On the other hand if $\eta < h_2(\mu)$ as in Fig. 4-B, the forward orbit of any point in $[f^{(L)^{-1}}(0), 0]$ is either contained in this interval (where f is monotone) or enters $[f(0), f^{(L)^{-1}}(0)]$ and approaches the stable two-cycle (this may be shown formally by the contraction mapping theorem). In any case, an n -cycle of f with $n \geq 3$ cannot include a point in $J = [f(0), 0]$.

Suppose for a contradiction f has an n -cycle with $n \geq 3$, call it $\{x_0 \dots x_{n-1}\} \subset [-\delta, \delta] \setminus J$. We now show that the restriction of f^2 to this n -cycle is a contraction giving a contradiction according to the contraction mapping theorem. Specifically we will argue that for any i and j ,

$$|f^2(x_j) - f^2(x_i)| < \frac{4}{9}|x_j - x_i|. \tag{30}$$

There are several cases to consider. For example, suppose that $x_j > 0$, $x_i < 0$ and $f^2(x_j) < f^2(x_i)$. Then $f(x_j) > f(0) - \frac{1}{3}x_j$ thus $f^2(x_j) > f(0) + \frac{1}{3}f(0) - \frac{1}{9}x_j$. Also $f(x_i) < f(0) - \frac{4}{3}x_i$ thus $f^2(x_i) < f(0) + \frac{1}{3}f(0) - \frac{4}{9}x_i$. Subtracting these inequalities leads to (30). The remaining cases can be shown similarly.

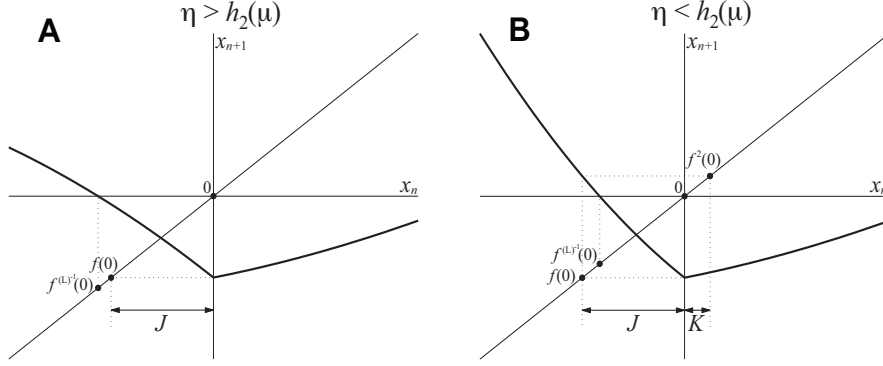


Figure 4: Schematic diagrams illustrating the map f , (8), when $\mu < 0$ and $\eta > h_2(\mu)$ in panel A and $\eta < h_2(\mu)$ in panel B. When $\eta = h_2(\mu)$, $f^{(L)-1}(0) = f(0)$.

Case III: $a_0^{(R)} > 0$.

Case IIIa: First suppose that $\mu \geq 0$. There exists $\delta_1 > 0$ such that whenever $\mu \in [0, \delta_1]$ and $\eta \in [-\delta_1, \delta_1]$, f is decreasing on $[-\delta_1, 0]$ and increasing on $[0, \delta_1]$. Since $\mu \geq 0$, $\forall x \in [-\delta_1, \delta_1]$, $f(x) \geq 0$. Thus any periodic solution of f in $[-\delta_1, \delta_1]$ must lie entirely in $[0, \delta_1]$. But f is increasing on this interval thus has no n -cycles with $n \geq 3$ here.

Case IIIb: Now suppose $\mu < 0$ and $\eta \geq h_2(\mu)$. There exists $\delta_2 > 0$ such that whenever $\mu \in [-\delta_2, 0)$ and $\eta \in [h_2(\mu), \delta_2]$, f is decreasing on $[-\delta_2, 0]$ and increasing on $[0, \delta_2]$, see Fig. 4-A. Suppose for a contradiction, f has an n -cycle with $n \geq 3$ on $[-\delta_2, \delta_2]$. Such an n -cycle must enter both $[-\delta_2, 0)$ and $(0, \delta_2]$, and so it includes a point $x \in (0, \delta_2]$ with $f(x) \in [-\delta_2, 0)$. But $f(x)$ lies in J , (29), and since $\eta \geq h_2(\mu)$, $f^2(0) \leq 0$, hence $f(J) \subset J$. Thus the forward orbit of x cannot return to $(0, \delta_2]$ which contradicts the assumption that x belongs to an n -cycle.

Case IIIc: Finally suppose $\mu < 0$, $\eta < h_2(\mu)$ and $0 < a_0^{(R)} < 1$. Then there exists $\delta_3 > 0$ such that whenever $\mu \in [-\delta_3, 0)$, $\eta \in [-\delta_3, h_2(\mu))$ and $x \in [-\delta_3, \delta_3]$,

$$-\left(1 + \frac{1 - a_0^{(R)}}{2(1 + a_0^{(R)})}\right) \leq f^{(L)'}(x) \leq -\frac{1}{2},$$

$$\frac{a_0^{(R)}}{2} \leq f^{(R)'}(x) \leq \frac{1 + a_0^{(R)}}{2},$$

where the particular non-symmetric $a_0^{(R)}$ -dependent bounds on the slopes have been chosen to simplify the subsequent analysis. Suppose for a contradiction f has an n -cycle with $n \geq 3$ in $[-\delta_3, \delta_3]$. As before, such an n -cycle must include a point $x \in (0, \delta_3]$ with $f(x) \in [-\delta_3, 0)$. Again $f(x) \in J$, but here $\eta < h_2(\mu)$, thus the forward orbit of x may return to the right of the origin but must enter the interval $K = [0, f^2(0)]$, see Fig. 4-B. Notice

$f^3(0) \leq f(0) + \frac{1+a_0^{(R)}}{2}f^2(0)$. Then by evaluating the first-order expansion of $f^{(L)}$ about $f(0)$ at $f^3(0)$, we arrive at $f^4(0) \geq f^2(0) - \left(1 + \frac{1}{2}\frac{1-a_0^{(R)}}{1+a_0^{(R)}}\right)\frac{1+a_0^{(R)}}{2}f^2(0) > 0$, therefore $f^2(K) \subset K$. Then $\forall y \in K$, $|f^2'(y)| \leq \left(1 + \frac{1}{2}\frac{1-a_0^{(R)}}{1+a_0^{(R)}}\right)\frac{1+a_0^{(R)}}{2} < 1$. Thus $f^2 : K \rightarrow K$ is a contraction mapping and therefore iterates of f that enter K cannot belong to an n -cycle with $n \geq 3$. Finally let $\delta = \min(\delta_1, \delta_2, \delta_3)$, then the result, (8), is proved.

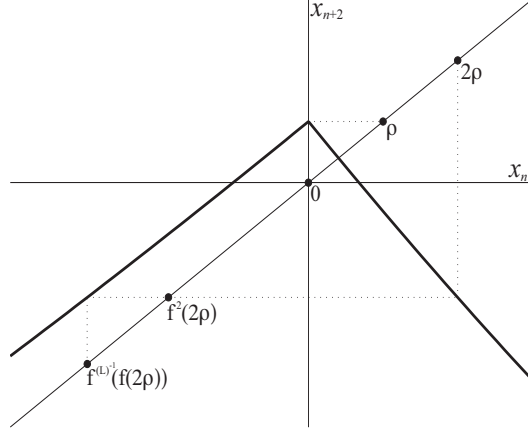


Figure 5: The second iterate of (2), f^2 , near $x = 0$ when $\mu < 0$, $\eta < h_2(\mu)$ and $a_0^{(R)} > 1$. The slope of this map is approximately unity left of the origin and approximately $-a_0^{(R)}$ right of the origin. As a consequence, see the text, the map exhibits chaos in $T = [f^{(L)^{-1}}(f(2\rho)), 2\rho]$.

Step 5: *Prove the existence of chaos when $\mu < 0$, $\eta < h_2(\mu)$ and $a_0^{(R)} > 1$.*

We first construct a trapping set, T , for f^2 . Let $\rho(\mu, \eta) = f^2(0; \mu, \eta)$. Since $\mu < 0$, by (28), $\rho(\mu, \eta) = O(2)$. Since $\eta < h_2(\mu)$, $\rho > 0$. Therefore

$$f(2\rho) = f(0) + (2a_0^{(R)} + O(1))\rho + O(\rho^2) < 0.$$

Consequently,

$$f^2(2\rho) = (1 - 2a_0^{(R)} + O(1))\rho + O(\rho^2), \quad (31)$$

$$f^{(L)^{-1}}(f(2\rho)) = (-2a_0^{(R)} + O(1))\rho + O(\rho^2). \quad (32)$$

Let

$$T = [f^{(L)^{-1}}(f(2\rho)), 2\rho],$$

It follows, see Fig. 5, that $\forall x \in T$, $f^2(2\rho) \leq f^2(x) \leq \rho$. But $\rho, f^2(2\rho) \in \text{int}(T)$, thus $f^2(T) \subset \text{int}(T)$, i.e. T is a trapping set for f^2 . Furthermore, $\bigcap_{i=0}^{\infty} f^{2i}(T)$, is an attracting set for f^2 .

Let $M \in \mathbb{Z}$ with $M \geq 2a_0^{(R)} + 2$. We now show that $\forall x \in T, \exists j \in \mathbb{Z}$ with $0 \leq j < M$ such that $f^{2j}(x) > 0$. Suppose otherwise. Then whenever $0 \leq j < M, f^{2j}(x) \leq 0$ and thus

$$f^{2j}(x) = (j + O(1))\rho + (1 + O(1))x + O(x^2). \quad (33)$$

Since f^2 is increasing on T_- , it suffices to consider $x = f^{(L)^{-1}}(f(2\rho))$. By combining (32) and (33) we find

$$\begin{aligned} f^{2(M-1)}(x) &\geq (2a_0^{(R)} + 1 + O(1))\rho + (1 + O(1))(-2a_0^{(R)} + O(1))\rho + O(\rho^2) \\ &= (1 + O(1))\rho + O(\rho^2) > 0, \end{aligned}$$

which is a contradiction.

Now consider the map $f^{2M} : T \rightarrow T$. Note that f^2 has one critical point on T , namely 0. Thus $y \in T$ is a critical point of f^{2M} if $f^{2j}(y) = 0$ for some $0 \leq j < M$. Consequently f^{2M} has at most $2^M - 1$ critical points, y_i , and f^{2M} is differentiable on T except at each y_i . For all $x \in T, x \neq y_i$,

$$f^{2M'}(x) = \prod_{j=0}^{M-1} f^{2'}(f^{2j}(x)).$$

Let $m \geq 1$ be the number of iterates, $f^{2j}(x)$, that are positive. Since left of zero the slope of f^2 is near 1 and right of zero the slope is near $-a_0^{(R)}$, we have

$$\left| f^{2M'}(x) \right| = a_0^{(R)m} + O(1) > \frac{1 + a_0^{(R)}}{2} > 1,$$

for any $x \neq y_i$, for sufficiently small μ, η . Consequently $f^{2M} : T \rightarrow T$ is *piecewise expanding* [34]. By the theorem of Li and Yorke [35], f^{2M} is chaotic on T . Thus f is chaotic on $T \cup f(T)$. \square

B Proof of Theorem 2

The theorem is proved in three steps. In the first two steps a center manifold, W^c , for the left half-map, $f^{(L)}$, is constructed and the lowest order terms of the restriction of $f^{(L)}$ to W^c are calculated. In the third step the two-cycle that has points in each half-plane is computed explicitly.

Step 1: *Compute W^c .*

It is convenient to extend the map to $\mathbb{R}^N \times \mathbb{R}^2$ by including the parameters in the extended phase space,

$$F = \begin{bmatrix} x' \\ \mu' \\ \eta' \end{bmatrix} = \begin{bmatrix} f^{(L)}(x; \mu, \eta) \\ \mu \\ \eta \end{bmatrix}.$$

Then

$$DF(0; 0, 0) = \left[\begin{array}{c|c|c} A_L(0, 0) & b(0, 0) & 0 \\ \hline 0 & 1 & 0 \\ 0 & 0 & 1 \end{array} \right],$$

has a three-dimensional center space

$$E^c = \text{span} \left\{ \begin{bmatrix} v(0,0) \\ 0 \\ 0 \end{bmatrix}, \begin{bmatrix} \varphi \\ 1 \\ 0 \end{bmatrix}, e_{N+2} \right\},$$

where

$$\varphi = (I - A_L(0,0))^{-1}b(0,0). \quad (34)$$

Notice

$$e_1^\top \varphi = \frac{\varrho^\top(0,0)b(0,0)}{\det(I - A_L(0,0))} \neq 0. \quad (35)$$

Since $e_1^\top v(0,0) = 1 \neq 0$, the center manifold, W^c , may be expressed locally in terms of s , μ and η . By the center manifold theorem, there exists a C^{k-1} function, H , such that on W^c

$$x = H(s; \mu, \eta) = sv(0,0) + \mu\zeta + O(2) \quad (36)$$

where

$$\zeta = \varphi - (e_1^\top \varphi)v(0,0). \quad (37)$$

Step 2: Determine an expression for $f^{(L)}$ on W^c and verify conditions (i)-(iii) of Theorem 1.

On W^c

$$\begin{aligned} s' &= e_1^\top f^{(L)}(H(s; \mu, \eta); \mu, \eta) \\ &= e_1^\top b(\mu, \eta)\mu + e_1^\top A_L(\mu, \eta)H(s; \mu, \eta) + e_1^\top g^{(L)}(H(s; \mu, \eta); \mu, \eta), \end{aligned} \quad (38)$$

where $g^{(L)}$ denotes all terms of $f^{(L)}$ that are nonlinear in x . With the given ‘‘hatted’’ variables (38) satisfies condition (ii) of Theorem 1 because

$$\begin{aligned} \left. \frac{\partial s'}{\partial \mu} \right|_{(0,0,0)} &= e_1^\top b(0,0) + e_1^\top A_L(0,0)\zeta \\ &= e_1^\top b(0,0) + e_1^\top A_L(0,0)\varphi - (e_1^\top \varphi)e_1^\top A_L(0,0)v(0,0) \quad (\text{by (37)}) \\ &= e_1^\top \varphi + (e_1^\top \varphi)e_1^\top v(0,0) \quad (\text{by (34)}) \\ &= 2e_1^\top \varphi, \end{aligned}$$

which with $\hat{\mu} = 2e_1^\top \varphi \mu$, in view of (35), produces

$$\left. \frac{\partial s'}{\partial \hat{\mu}} \right|_{(0,0,0)} = 1.$$

A similar verification of (i) and (iii) of Theorem 1 is now given. By scaling v , we may assume that for small η , $e_1^\top v(0, \eta) \equiv 1$. Since (36) lacks a linear η term,

$$H(s; 0, \eta) = v(0, \eta)s + O(s^2),$$

and consequently

$$\begin{aligned} s'|_{\mu=0} &= e_1^\top A_L(0, \eta)v(0, \eta)s + O(s^2) \\ &= \lambda(0, \eta)s + O(s^2). \end{aligned}$$

Thus

$$\begin{aligned}\frac{\partial s'}{\partial s}\Big|_{(0;0,0)} &= \lambda(0,0) = -1, \\ \frac{\partial^2 s'}{\partial \eta \partial s}\Big|_{(0;0,0)} &= \frac{\partial \lambda}{\partial \eta}(0,0) = 1,\end{aligned}$$

as required.

Step 3: *Compute the two-cycle that has points in each half-plane to verify the final statement of the theorem.*

We have

$$f^{(L)}(f^{(R)}(x; \mu, \eta); \mu, \eta) = (I + A_L(0, \eta))b(0, \eta)\mu + A_L(0, \eta)A_R(0, \eta)x + O(|\mu, x|^2). \quad (39)$$

By applying the implicit function theorem to (39) in view of condition (v) of the theorem we see that the two-cycle with points in each half-plane exists and is unique for small μ and η . When admissible, the point of this cycle in the right half-plane is given by a C^k function

$$x^{*(RL)}(\mu, \eta) = (I - A_L A_R)^{-1}(I + A_L)b\Big|_{\mu=0} \mu + O(\mu^2).$$

Then

$$\begin{aligned}\frac{\partial s^{*(RL)}}{\partial \mu}\Big|_{\mu=0} &= e_1^\top (I - A_L A_R)^{-1}(I + A_L)b\Big|_{\mu=0} \\ &= \frac{e_1^\top \text{adj}(I - A_L A_R)(I + A_L)b}{\det(I - A_L A_R)}\Big|_{\mu=0}.\end{aligned}$$

Since $I - A_L A_R = (I + A_L)(I - A_R) - A_L + A_R$ and A_L and A_R are identical in their last $N - 1$ columns, $\text{adj}(I - A_L A_R)$ and $\text{adj}((I + A_L)(I - A_R))$ share the same first row. Thus

$$\begin{aligned}\frac{\partial s^{*(RL)}}{\partial \mu}\Big|_{\mu=0} &= \frac{e_1^\top \text{adj}(I - A_R)\text{adj}(I + A_L)(I + A_L)b}{\det(I - A_L A_R)}\Big|_{\mu=0} \\ &= \frac{\det(I + A_L)}{\det(I - A_L A_R)} \varrho^\top b\Big|_{\mu=0} \\ &= \frac{\frac{\partial}{\partial \eta} \det(I + A_L)}{\det(I - A_L A_R)} \varrho^\top b\Big|_{(0,0)} \eta + O(\eta^2).\end{aligned}$$

By Theorem 1, there exists a C^{k-2} curve, $\hat{\eta} = h_2(\hat{\mu})$, along which, $s^{*(RL)} = 0$. Furthermore, when $\hat{\mu} \leq 0$, the two-cycle is admissible along this curve. If $\tilde{\eta} = \eta - h_2(\hat{\mu})$, then

$$s^{*(RL)}(\hat{\mu}, \tilde{\eta}) = \frac{\det(I - A_L) \frac{\partial}{\partial \eta} \det(I + A_L)}{2 \det(I - A_L A_R)}\Big|_{(0,0)} \hat{\mu} \tilde{\eta} + O(3),$$

which confirms the final statement of the theorem. \square

References

- [1] Z.T. Zhusubaliyev and E. Mosekilde. *Bifurcations and Chaos in Piecewise-Smooth Dynamical Systems*. World Scientific, Singapore, 2003.
- [2] S. Banerjee and G.C. Verghese, editors. *Nonlinear Phenomena in Power Electronics*. IEEE Press, New York, 2001.
- [3] C.K. Tse. *Complex Behavior of Switching Power Converters*. CRC Press, Boca Raton, FL, 2003.
- [4] R.I. Leine and H. Nijmeijer. *Dynamics and Bifurcations of Non-smooth Mechanical systems*, volume 18 of *Lecture Notes in Applied and Computational Mathematics*. Springer-Verlag, Berlin, 2004.
- [5] K. Popp. Non-smooth mechanical systems. *J. Appl. Math. Mech.*, 64(5):765–772, 2000.
- [6] M. Wiercigroch and B. De Kraker, editors. *Applied Nonlinear Dynamics and Chaos of Mechanical Systems with Discontinuities.*, Singapore, 2000. World Scientific.
- [7] B. Brogliato. *Nonsmooth Mechanics: Models, Dynamics and Control*. Springer-Verlag, New York, 1999.
- [8] J. Awrejcewicz and C. Lamarque. *Bifurcation and Chaos in Nonsmooth Mechanical Systems*. World Scientific, Singapore, 2003.
- [9] T. Puu and I. Sushko, editors. *Business Cycle Dynamics: Models and Tools*. Springer-Verlag, New York, 2006.
- [10] E. Mosekilde and J.L. Laugesen. Nonlinear dynamic phenomena in the beer model. *Syst. Dyn. Rev.*, 23:229–252, 2007.
- [11] J. Caballé, X. Jarque, and E. Michetti. Chaotic dynamics in credit constrained emerging economies. *J. Econ. Dyn. Control*, 30:1261–1275, 2006.
- [12] M. di Bernardo, C.J. Budd, A.R. Champneys, and P. Kowalczyk. *Piecewise-smooth Dynamical Systems. Theory and Applications*. Springer-Verlag, New York, 2008.
- [13] Z.T. Zhusubaliyev, E. Mosekilde, S. Maity, S. Mohanan, and S. Banerjee. Border collision route to quasiperiodicity: Numerical investigation and experimental confirmation. *Chaos*, 16(2):023122, 2006.
- [14] I. Sushko and L. Gardini. Center bifurcation for a two-dimensional piecewise linear map. In T. Puu and I. Sushko, editors, *Business Cycle Dynamics: Models and Tools.*, pages 49–78. Springer-Verlag, New York, 2006.
- [15] D.J.W. Simpson and J.D. Meiss. Neimark-Sacker bifurcations in planar, piecewise-smooth, continuous maps. *SIAM J. Appl. Dyn. Sys.*, 7(3):795–824, 2008.

- [16] S. Banerjee and C. Grebogi. Border collision bifurcations in two-dimensional piecewise smooth maps. *Phys. Rev. E*, 59(4):4052–4061, 1999.
- [17] M. Dutta, H.E. Nusse, E. Ott, J.A. Yorke, and G. Yuan. Multiple attractor bifurcations: A source of unpredictability in piecewise smooth systems. *Phys. Rev. Lett.*, 83(21):4281–4284, 1999.
- [18] D.J.W. Simpson. *Bifurcations in Piecewise-Smooth, Continuous Systems*. PhD thesis, The University of Colorado, 2008.
- [19] D.J.W. Simpson, D.K. Kompala, and J.D. Meiss. Discontinuity induced bifurcations in a model of *Saccharomyces cerevisiae*. *Math. Biosci.*, 218(1):40–49, 2009.
- [20] A. Colombo and F. Dercole. Discontinuity induced bifurcations of non-hyperbolic cycles in nonsmooth systems. Submitted to: *SIAM J. Appl. Dyn. Sys.*
- [21] M. di Bernardo, C.J. Budd, and A.R. Champneys. Corner collision implies border-collision bifurcation. *Phys. D*, 154:171–194, 2001.
- [22] F. Angulo, M. di Bernardo, S.J. Hogan, P. Kowalczyk, and G. Olivar. Two-parameter non-smooth bifurcations in power converters. *IEEE Int. Symp. Circ. Syst.*, pages 1485–1488, 2005. Kobe, Japan, 23-26 May.
- [23] F. Angulo, G. Olivar, and M. di Bernardo. Two-parameter discontinuity-induced bifurcation curves in a ZAD-strategy-controlled DC-DC buck converter. *IEEE Trans. Circuits Systems I Fund. Theory Appl.*, 55(8):2392–2401, 2008.
- [24] M. di Bernardo, P. Kowalczyk, and A. Nordmark. Bifurcations of dynamical systems with sliding: Derivation of normal-form mappings. *Phys. D*, 170:175–205, 2002.
- [25] P. Kowalczyk, M. di Bernardo, A.R. Champneys, S.J. Hogan, M. Homer, P.T. Piiroinen, Yu.A. Kuznetsov, and A. Nordmark. Two-parameter discontinuity-induced bifurcations of limit cycles: Classification and open problems. *Int. J. Bifurcation Chaos*, 16(3):601–629, 2006.
- [26] M. di Bernardo, C.J. Budd, and A.R. Champneys. Normal form maps for grazing bifurcations in n -dimensional piecewise-smooth dynamical systems. *Phys. D*, 160:222–254, 2001.
- [27] G. Osorio, M. di Bernardo, and S. Santini. Corner-impact bifurcations: A novel class of discontinuity-induced bifurcations in cam-follower systems. *SIAM J. Appl. Dyn. Sys.*, 7(1):18–38, 2008.
- [28] C.J. Budd and P.T. Piiroinen. Corner bifurcations in non-smoothly forced impact oscillators. *Phys. D*, 220:127–145, 2006.
- [29] R.I. Leine and D.H. Van Campen. Discontinuous bifurcations of periodic solutions. *Math. Comput. Model.*, 36:259–273, 2002.

- [30] S.K. Berberian. *Linear Algebra*. Oxford University Press, New York, 1992.
- [31] B. Kolman. *Elementary Linear Algebra*. Prentice Hall, Upper Saddle River, NJ, 1996.
- [32] M. di Bernardo, M.I. Feigin, S.J. Hogan, and M.E. Homer. Local analysis of C -bifurcations in n -dimensional piecewise-smooth dynamical systems. *Chaos Solitons Fractals*, 10(11):1881–1908, 1999.
- [33] J. Guckenheimer and P.J. Holmes. *Nonlinear Oscillations, Dynamical Systems, and Bifurcations of Vector Fields*. Springer-Verlag, New York, 1986.
- [34] R.C. Robinson. *An Introduction to Dynamical Systems. Continuous and Discrete*. Prentice Hall, Upper Saddle River, NJ, 2004.
- [35] T. Li and J.A. Yorke. Ergodic transformations from an interval into itself. *Trans. Amer. Math. Soc.*, 235(1):183–192, 1978.